Biomedical Engineering Advances 9 (2025) 100139

Contents lists available at ScienceDirect

Biomedical Engineering Advances

journal homepage: www.journals.elsevier.com/biomedical-engineering-advances

New MAO coatings on multiprincipal equimassic β TiNbTaZr and TiNbTaZrMo alloys

Rafael F.M. dos Santos [a], Pedro A.B. Kuroda [b,*], Gerson S. de Almeida [c], Willian F. Zambuzzi [c], Carlos R. Grandini [d], Conrado R.M. Afonso [a]

[a] UFSCar – Universidade Federal de São Carlos, Materials Engineering Department (DEMa), 13565-905, São Carlos, SP, Brazil
[b] UNILA – Universidade Federal da Integração Latino-Americana, 85870-650, Foz do Iguaçu, PR, Brazil
[c] UNESP – Universidade Estadual Paulista, Laboratory of Bioassays and Cellular Dynamics, Department of Chemical & Biological Sciences, Institute of Biosciences, 18618-687, Botucatu, SP, Brazil
[d] UNESP – Universidade Estadual Paulista, Laboratório de Anelasticidade e Biomateriais, 17033-360, Bauru, SP, Brazil

ARTICLE INFO

Keywords:
β HEA alloys
MAO
Surface characterization
Multiprincipal equimassic alloys

ABSTRACT

β titanium alloys are essential in biomedical applications due to their combination of high strength, low elastic modulus, and biocompatibility. Although high-entropy alloys (BioHEAs) containing Nb, Zr, Ta, and Mo offer high mechanical strength, their elevated elastic modulus can lead to stress shielding in orthopedic applications. To address these limitations, β-stable alloys with enhanced mechanical and surface properties are being developed to support osseointegration and cellular adhesion. The work focuses on innovative medium (MEA) and high entropy (HEA) equimassic β Ti alloys (quaternary Ti-25Ta-25Nb-25Zr and quinary Ti-20Zr-20Ta-20Nb-20Mo in wt.%) treated with micro-arc oxidation (MAO) to optimize their performance as biomaterials. The MAO process generated bioactive coatings enriched with Ca, P, and Mg, promoting bone cell proliferation. X-ray diffraction (XRD) identified β phase structures and revealed amorphous or partially crystalline coatings, with a ZrO_2 cubic phase noted in the MEA quaternary Ti-25Ta-25Nb-25Zr alloy. Surface morphology assessments showed porous and lamellar topographies that varied with alloy composition, resulting in increased hydrophilicity and optimal roughness. Confocal microscopy confirmed that the MAO coating thickness on MEA quaternary Ti-25Ta-25Nb-25Zr (10.4 μm) surpassed that on HEA (high entropy alloy) quinary Ti-20Zr-20Ta-20Nb-20Mo (4.2 μm). Cell viability and adhesion assays indicated significant biocompatibility, particularly for MEA (medium entropy alloy) quaternary Ti-25Ta-25Nb-25Zr, which benefits from a Mo-free composition. These results underscore the potential of these multiprincipal equimassic bcc (body centered cubic) β alloys for biomedical applications, possibly enhancing osteoblast attachment and sustain cell viability effectively.

1. Introduction

The search for solutions to address tissue and organ malfunctions due to accidents, diseases, or aging has driven the research into new materials for prosthetics and implants [1–4]. The development of β titanium alloys (β-Ti), introduced into the biomedical industry in the 1990s, aims to improve quality of life. Initially, the focus was on biocompatibility, but today, it extends to osseointegration, bioactivity, corrosion resistance, mechanical strength, and the reduction of the elastic modulus (E, GPa) [5–11].

Recently, equiatomic high-entropy alloys (BioHEA), composed of non-toxic elements such as Niobium (Nb), Zirconium (Zr), Tantalum (Ta), and Molybdenum (Mo), have demonstrated higher mechanical strength compared to traditional alloys, such as those in the Ti-Nb and Ti-Nb-Zr systems [12–14]. However, the increase in the elastic modulus is undesirable in orthopedic implants, as it can cause stress shielding [15–19]. Thus, alloys with equimassic composition may offer better mechanical strength and biocompatibility (lower elastic modulus $E = 50$ – 80 GPa) compared to traditional β-Ti alloys while having a Young modulus closer to that of human bone ($E = 30$ GPa) than BioHEAs, due to their lower fractions (wt.%) of refractory elements such as Mo and Ta, compared to BioHEAs [20]. However, in addition to enhancing the bulk

* Corresponding author at: Universidade Federal da Integração Latino-Americana, Avenida Tarquínio Joslin dos Santos, 1000 - Polo Universitário, 85870-650, Foz do Iguaçu, PR, Brazil.

E-mail address: pedro.kuroda@ufscar.br (P.A.B. Kuroda).

https://doi.org/10.1016/j.bea.2024.100139
Received 17 October 2024; Received in revised form 19 November 2024; Accepted 6 December 2024
Available online 12 December 2024

properties of the material, it is also crucial to improve the surface properties of the developed alloys.

The biomaterial's surface plays a crucial role in the interaction of the implant with the biological environment [21]. Titanium alloys, being bioinert, face challenges in forming surface oxides, which can result in low cellular adhesion compared to bioactive materials [22]. To overcome these limitations, the biofunctionalization of titanium surfaces is an effective approach to enhance bone cell adhesion and proliferation [23]. The bioactivity of the surface is influenced by factors such as topography, porosity, microstructure, and chemical composition [24]. The primary techniques for surface modification include electrodeposition [25], micro-arc oxidation (MAO) [26,27], and anodization [28].

MAO is a straightforward technique that does not require significant investment in equipment, which has contributed to the increasing number of studies utilizing this method [26,29]. The morphology and performance of micro-arc oxide coatings are influenced by the electrolyte's composition (including additives and pH) and operational parameters such as current, voltage, pulse duration, and processing time [9,30,31]. An anodic coating produced by the MAO process significantly improves the surface properties of Ti alloys for use in the biomedical field; the ceramic coating (usually consisting of TiO2) improves corrosion resistance [32] and improves wear resistance since ceramic materials tend to have greater chemical stability than metals [33]. In addition, the MAO coating can be performed in a biomimetic conductive electrolyte solution containing elements essential for the growth and formation of bone tissue, such as calcium, phosphorus, and magnesium [34].

Recent literature reports the use of the MAO technique to improve the biocompatibility, wear resistance, and corrosion of Ti alloys [9]. Another widely studied approach is the addition of small amounts of elements harmful to human health, such as Cu, Zn, and Ag, to the coating's surface layer [35–38], so that they act as a bactericidal agent and do not promote host cell death. The concentrations of these elements must be controlled for this.

Equimassic or multi-principal element alloys (Ti-25Nb-25Zr-25Ta and Ti-20Nb-20Zr-20Ta-20Mo) form a new class of high or medium-entropy alloys manufactured for the biomedical field. Unlike equiatomic high entropy alloys, where the element a with the highest atomic mass has a greater amount in weight percentage in the alloy, equimassic alloys are classified as multicomponent alloys without a majority presence (weight fraction) of a metallic element in the alloy. They may have low values of elastic modulus of 73 ± 2 GPa (25Ta) and 88 ± 2 GPa (20Mo), as dos Santos presented [39]. In the current literature, it is possible to find studies that produce high and medium entropy alloys with and without anodic coating, such as Ti-Ta-Zr-Nb [16,40], Ti-Nb-Ta-Zr-Hf [41], Ti-Nb-Zr [42,43] and Ti-Ta-Zr [18,44]. In addition to producing an MAO layer, our studies, due to the oxidation of the alloying elements, incorporated the elements calcium, phosphorus, and magnesium in the coating in order to improve the biocompatibility of the materials produced. The production of MAO coatings rich in bioactive elements produced in the Ti-25Nb-25Zr-25Ta and Ti-20Nb-20Zr-20Ta-20Mo alloys has not yet been reported in the literature.

Due to the advantages of producing new Ti alloys for biomedical purposes and the favorable qualities that the MAO technique promotes in metal implants, this work aims to produce new equimassic β alloys (Ti-20Zr-20Ta-20Nb-20Mo and Ti-25Ta-25Nb-25Zr) with the surface functionalized by the MAO technique, superficially incorporating the elements Ca, P, and Mg.

2. Material and methods

Ingots (30 g) of the equimassic Ti alloys, Ti-25Nb-25Zr-25Ta and Ti-20Nb-20Zr-20Ta-20Mo (wt.%), were produced using an arc melting furnace in a water-cooled copper crucible, employing a non-consumable tungsten electrode and a controlled argon atmosphere [45].

After preparing the ingots, the materials were sanded with 600 mesh wet sandpaper to standardize the surface before performing MAO anodic oxidation. MAO treatments were performed in a DC power source (Keysight, N5751A) at 300 V, with a limited current of 2.5 A, at room temperature, for 60 s. The electrolyte consisted of 0.35 M calcium acetate monohydrate ($(CH_3COO)_2Ca \cdot H_2O$), 0.02 M β-glycerol phosphate ($C_3H_7Na_2O_6P \cdot 5H_2O$), and 0.1 M magnesium acetate tetrahydrate ($C_4H_6MgO_4$ $4H_2O$) [46] to enable the incorporation of the bioactive elements Ca, P, and Mg, which are considered essential for bone recovery and strengthening.

X-ray photoelectron spectroscopy (XPS) was conducted to analyze the oxides present in the MAO layer using a Thermo Kα XPS system (Thermo Scientific, Inc.). The instrument utilized a monochromatic X-ray source with an aluminum anode (Kα = 1.486 eV). A spot size of 400 μm was used, with an energy step of 200 eV for wide-energy scans. The resolution was set at 1 eV for long scans and 0.01 eV for short scans, covering an energy range from 0 to 1300 eV

The crystal structure of the metal bulks and MAO coatings were characterized using an X-ray diffractogram (XRD) with a Bruker D8 Advanced-ECO Diffractometry with Cu-Kα radiation with 2θ = 10 to 90°. The microstructure of the metals and the MAO layer were analyzed using a scanning electron microscope - SEM from Carl Zeiss Inc. A confocal laser scanning microscope - CLSM from Leica, model DC3 M, was used to determine the roughness of the MAO coatings [46].

Wettability and surface energy were obtained using contact angle measurements by the droplet technique on a Krüss DSHAT HTM Reetz GmbH goniometer.

Vickers microhardness analysis was performed using a load of 0.5 kgf (4.90 N) for 15 s in a Shimadzu HMV-2 equipment [47]. Wettability was evaluated using contact angle measurements and the droplet technique on a Krüss (HTM Reetz GmbH). Deionized water (polar liquid), 2.5 μl volume, was used as the test fluid.

Cell viability and adhesion tests were performed as part of the initial cytotoxicity assessments. Discs (10×10×3 mm^3) were used to evaluate the cytotoxic potential of the alloys under investigation. Three samples of each alloy were used for the tests, which were carried out in triplicate. Pre-osteoblastic cells, MC3T3-E1, subclone 4, were cultured in α-minimum essential medium (α-MEM) supplemented with 10% fetal bovine serum (FBS) and antibiotics (penicillin 100 U/mL and streptomycin 100 mg/mL). The cultures were maintained in an incubator at 37 °C with 5% CO_2 until plate confluence was reached. Conventional cultures, without any treatment, were used as reference control to further investigate the cytotoxicity of the Ti alloys.

The cytotoxicity evaluation was performed considering the indirect effect of Ti alloys by incubating the Ti alloys in cell culture medium up to 24 h into incubator at 37 °C. Thereafter, the conditioned medium was used to treat the cells, in agreement with ISO 10,993: 2016 guidelines. Prior to use, this conditioned medium was properly supplemented with FBS 10% and used to challenge the pre-osteoblasts up to 24 h in conventional conditions. Previously, the cells were plated 24 h before treatment in a 96-well plate at a 5×10^4 cells/mL density, when the cell viability was measured using a standard marker 3-(4,5-dimethylthiazol-2-yl)−2,5-diphenyltetrazolium bromide (MTT) (Sigma Aldrich #M5455–1 G). The culture medium was removed, and 1 mg/mL of MTT was added to the cultures and incubated for additional 3 h, when the medium was removed, and 0.1 mL of dimethyl sulfoxide (DMSO) was added to solubilize the dye formed by viable cells. Absorbance was then measured at 570 nm using a microplate reader.

Additionally, for the cell adhesion evaluation, pre-osteoblasts were treated and plated using the Ti alloy-conditioned medium for 24 h. Thereafter, the cells were trypsinized, counted, and reseeded in 96-well plates at a 5×10^4 cells/mL density. After 24 h of seeding, the adherent cells were washed with phosphate-buffered saline (PBS) at 37 °C and fixed in absolute ethanol-glacial acetic acid (3:1, v/v) for 10 min at room temperature. The adherent cells were stained with 0.1% crystal violet (w/v) for 10 min. Excess dye was removed by decantation, and the cells were washed twice with distilled water. Dye extraction was performed using 10% (v/v) acetic acid, and absorbance was measured at 540 nm using a microplate reader.

3. Results and discussions

Table 1 shows the semi-quantitative chemical composition results obtained by the EDS technique of the alloys produced in this work. It can be observed that the chemical elements (Ti, Ta, Mo, Nb, and Zr) were satisfactorily detected in the alloys produced, and the experimental values are similar to the nominal values (25 and 20% by weight for the quinary and quaternary alloys, respectively). The chemical composition determined via EDS has an error of approximately 2% by weight for the alloying elements, which may explain the small changes in the values obtained.

After the alloys were produced, anodic oxidation (MAO) was performed to functionalize the surface of the alloys with a coating resulting from the oxidation of the alloying elements enriched with functional agents, such as calcium, phosphorus, and magnesium. The results of the chemical composition, via XPS and EDS, of the coatings are presented in Fig. 1.

The XPS results showed that the MAO coating comprises the oxidized bulk elements Ti, Zr, Nb, and Ta in both alloys and the additional Mo in the Ti-20Nb-20Zr-20Ta-20Mo alloy. It is observed that in the quaternary alloy, there is a greater quantity of the elements Ti, Zr, Ta, and Nb in the coatings since in this alloy, there is a greater quantity of these elements in the metallic bulk, since Mo acted as a substitutional element, removing 5% by weight of each element in the alloy. In addition, it is noted that the elements Ca, P, and Mg were successfully incorporated into the coatings, with the additional carbon from the acetates used in the electrolytic solution.

The EDS technique also determined the chemical composition of the coating. It can be seen that the EDS technique detects a higher concentration of metals originating from the substrate (Ti, Ta, Zr, Nb, and Mo) because the penetration of the electron beam of the electron microscope has a penetration of around a few micrometers (greater than the average thickness of anodic films produced in Ti alloys), obtaining results of the film composition together with the chemical information of the metal substrates. On the other hand, XPS has a penetration of a few nanometers and does not penetrate the substrate, which is the most reliable analysis to determine the chemical composition of the anodic oxide. In addition, the EDS technique is ineffective in quantifying the chemical composition of light elements such as oxygen and carbon.

X-ray diffraction measurements were conducted to identify the crystalline phases in the metal substrates and MAO coatings, as shown in Fig. 2. It can be observed that both alloys produced are of the β type, with a body-centered cubic crystal structure. Ti and Zr are alloy elements with a hexagonal compact crystal structure, known as α, where the β phase can be reached at high temperatures (~850 °C). However, some elements known as β-stabilizers promote the decrease in the allotropic transformation temperature of Ti and Zr. Among these elements are Nb, Ta, and Mo, which are considered isomorphic β -stabilizers because they do not promote the formation of intermetallic phases. Due to the high amounts of Nb, Mo, and Ta, the alloys produced in this work are β-stable. Some studies also report the weak β-stabilizing action of Zr in Ti alloys containing Nb, Ta, or Mo [18].

Table 1
Nominal chemical composition of the bcc MEA Ti-25Nb-25Zr-25Ta and HEA Ti-20Nb-20Zr-20Ta-20Mo equimassic β-Ti alloys in weight percentage (wt.%), in atomic percentage (at.%), the semi-quantitative analysis via MEV-EDS (wt.%).

Nominal Composition (wt.%)	Nominal Composition (at.%)	Composition (EDS, wt.%)
Ti-25Nb-25Zr-25Ta	$Ti_{43,4}Nb_{22,4}Zr_{22,7}Ta_{11,5}$	Ti-25Nb-24Zr-26Ta
Ti-20Nb-20Zr-20Ta-20Mo	$Ti_{35,7}Nb_{18,4}Zr_{18,7}Ta_{9,4}Mo_{17,8}$	Ti-20Nb-21Zr-20Ta-19Mo

Regarding the X-ray diffraction patterns obtained on the surface of the alloys oxidized via MAO, the coatings are basically amorphous, evidenced by the characteristic halo of amorphous materials. Several studies show that MAO coatings are mostly amorphous due to the high temperatures reached by the sparks (electric arcs) that promote the oxidation of the metals [48]. The coatings are grown inside an electrolytic cell that rapidly cools the oxidized material, not providing enough energy and time for the oxide atoms to regroup to form an ordered three-dimensional structure. Therefore, the quinary alloy has a completely amorphous MAO coating, while the quaternary alloy has only one crystalline phase: cubic zirconium dioxide (ZrO_2). Possible detection of crystalline oxide of Zr or Ti was expected since these two elements are in group 4 of the periodic table and have high reactivity with oxygen, being able to form stable oxides.

The ZrO_2 oxide, like TiO_2, presents three distinct (allotropic) crystalline phases: monoclinic (stable at temperatures up to 1000 °C), tetragonal (stable at temperatures between 1000 and 1500 °C), and cubic (stable at temperatures above 1500 °C). It is observed that the MAO coating produced on the Ti-25Nb-25Zr-25Ta alloy contains the ZrO_2 phase that is stable at high temperatures. This formation is due to the high voltage (300 V) and current applied during the MAO process (2.5 A), since high voltages and current promote the formation and nucleation of high-energy phases, as indicated by Attarzadeh and Ramana [49].

From the diffraction data, the lattice parameter of the β phase of the substrate and the cubic phase of ZrO_2 were calculated by Bragg's law, where the quaternary alloy Ti-25Nb-25Zr-25Ta has a bcc lattice parameter of $a = 3.36$ Å and the Ti-20Nb-20Zr-20Ta-20Mo alloy has a β phase (bcc structure) with a lower lattice parameter ($a = 3.31$ Å). The lower value of the lattice parameter of the β phase of the Ti-20Nb-20Zr-20Ta-20Mo alloy is due to the addition of Mo, which has the lowest atomic radius (1.3 Å) compared to Ti (1.47 Å), Zr (1.60 Å), Ta (2.00 Å) and Nb (1.43 Å). The lattice parameter of the cubic phase of ZrO_2 is approximately 5.05 Å and is like other values found in the literature [50, 51].

Fig. 3 shows the micrographs of the metallic bulks and the MAO coatings. The alloys exhibit a dendritic microstructure, which is characteristic of materials in the as-cast condition and medium- (MEA) and high-entropy alloys (HEA). The images clearly show significant segregation between the dendrite core and the surrounding interdendritic regions. This elemental distribution arises from solidification, where elements with lower melting points, such as Ti and Zr, solidify earlier, concentrating in the dendrite cores (appearing as dark regions). Meanwhile, elements with higher melting points, like Nb and Ta, segregate into the interdendritic zones during solidification (visible as light regions).

The topographic images of the MAO coatings show porous structures characteristic of anodic surfaces made of Ti and Zr alloys. Small circular micropores and lamellae are present on the surface of the alloys. When the applied voltage exceeds the dielectric limit of the oxide film that forms on the material's surface, localized electrical discharges (microarcs) occur that pierce this oxide layer. These discharges create small cavities on the surface, giving rise to micropores. The energy released in the discharges creates regions of high temperature and pressure plasma. The formation of micropores is influenced by the rapid solidification of the molten material when the discharge ceases.

It is noted that the topographic morphology of the MAO coatings is different; for Ti-20Nb-20Zr-20Ta-20Mo (20Mo) alloy, there is micropores formation, while for Ti-25Nb-25Zr-25Ta (25Ta), there is the formation of a porous oxide with a lamellar shape. Kuroda et al. performed the MAO surface modification on new β-Ti alloys (Ti-25Ta-Zr-Nb) and showed that in the alloy with the largest amount of β-stabilizing elements (Ta, Zr, and Nb), there is the formation of MAO coatings with similar lamellar structures [40]. It seems that, for HEA Ti-20Nb-20Zr-20Ta-20Mo (20Mo) alloy, the MAO coating characteristic

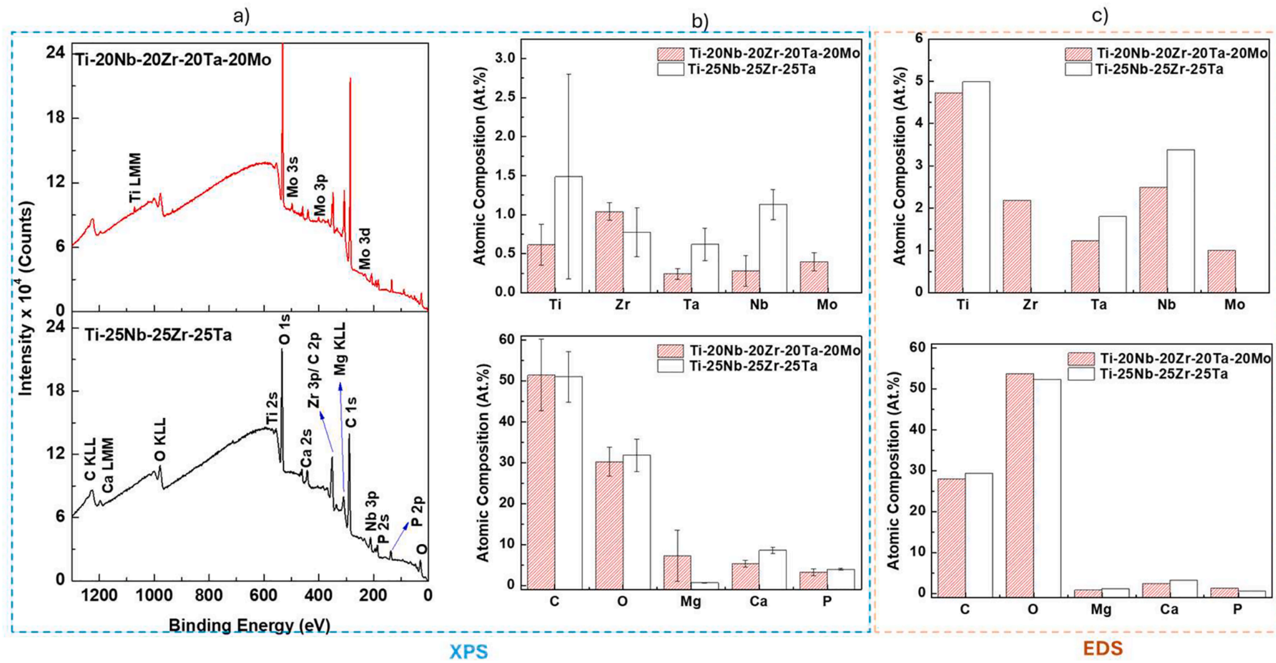

Fig. 1. Spectra (a) and chemical composition (b) of the MAO coating obtained by XPS technique. Chemical composition of the MAO coating obtained by EDS (c).

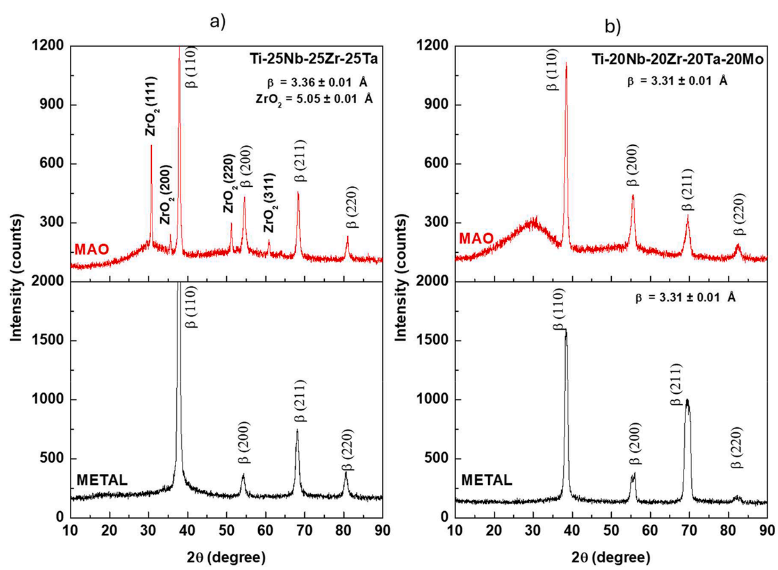

Fig. 2. X-ray diffraction patterns obtained for the multiprincipal bcc MEA quaternary Ti-25Nb-25Zr-25Ta (a) and HEA quinary Ti-20Nb-20Zr-20Ta-20Mo (b) alloys, before and after the MAO process.

tend to back to micropores formation.

Various biocompatible materials with distinct characteristics are required in the biomedical field for a given application. For example, metals are widely used in dentistry, orthopedics, and the cardiovascular area. A metal used as an orthopedic implant to repair a bone fracture must have a rough surface with micropores rich in calcium, phosphorus, and magnesium (as in this work) to promote good adhesion of bone tissue cells (osteoblasts) to the metal implant and promote cell growth around the implant. On the other hand, this same material, with the same characteristics, is not required in the cardiovascular area as a valve implant since a rough surface promotes blood clotting. A smooth and hydrophobic surface is ideal in this type of application (cardiovascular).

Fig. 4 shows the cross-sectional image. The image shows the thickness of the MAO coatings, with the Ti-25Nb-25Zr-25Ta alloy film being thicker than the Ti-20Nb-20Zr-20Ta-20Mo alloy film, with values of 10.4 µm and 4.2 µm, respectively. Ti, Nb, Ta, and Nb are valve metals. They can form passive oxide layers when subjected to anodic polarization, unlike Mo. Forming a stable oxide under the usual electrolytic conditions is impossible on the Mo substrate. On the Mo surface, when subjected to the MAO process, soluble or unstable oxides tend to form, which do not adhere to the substrate. Cardoso produced MAO coatings on a Ti alloy containing Mo (Ti-30Nb-5Mo), and his XPS chemical composition results showed that Ti oxide (TiO_2) and Nb (Nb_2O_5) were formed on the metal surface. Still, Mo oxide was not detected in the MAO coating [36]. In this work, as the Mo element acts as a substitutional element, the quinary alloy has a smaller amount of valve metals; due to this, the MAO film produced in the Ti-20Nb-20Zr-20Ta-20Mo alloy has a smaller thickness.

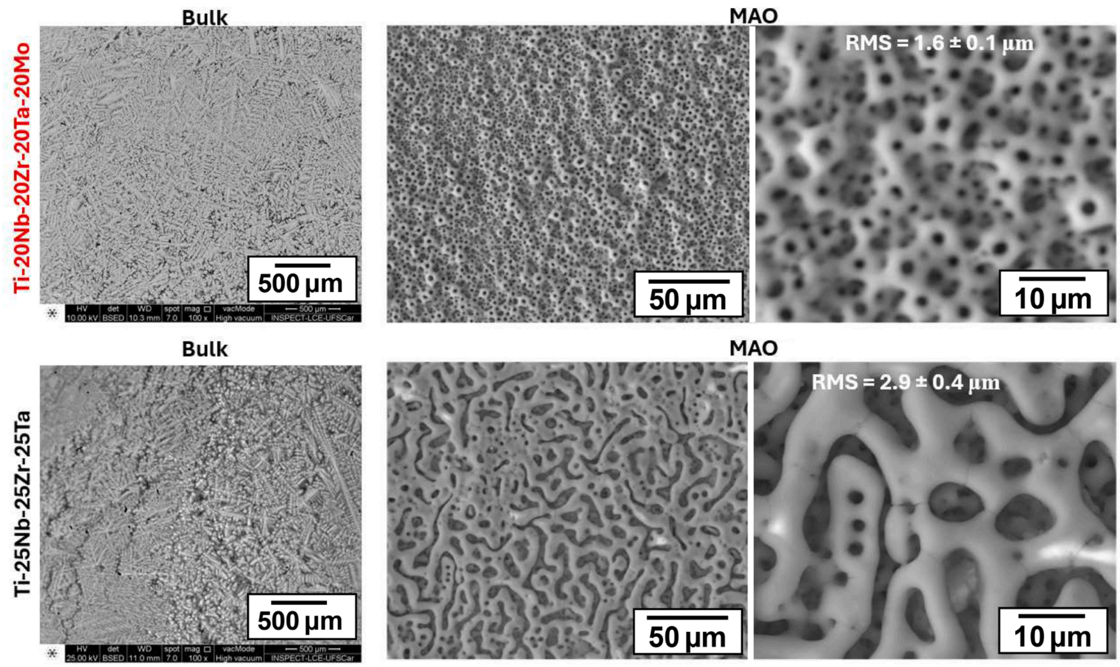

Fig. 3. SEM Micrographs in BSE signal of the HEA Ti-20Nb-20Zr-20Ta-20Mo and MEA Ti-25Nb-25Zr-25Ta equimassic alloys before and after the MAO process.

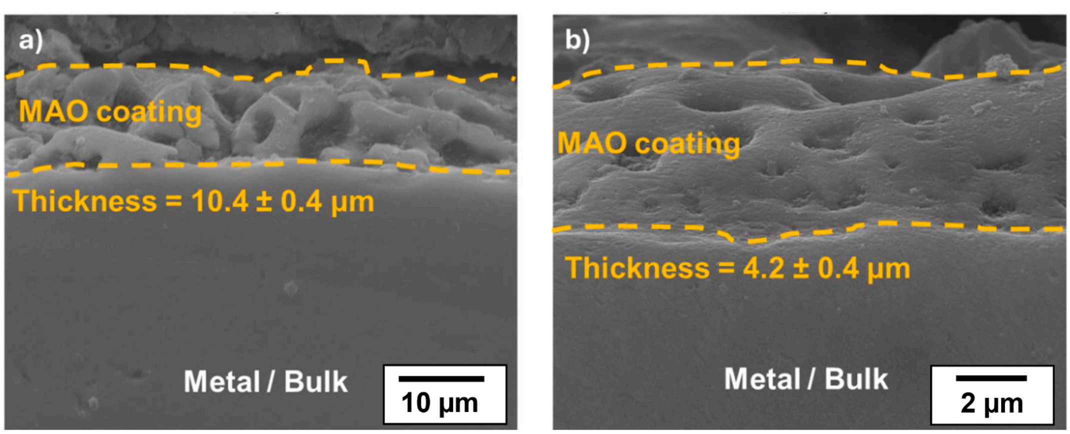

Fig. 4. SEM images of the cross-section of the multiprincipal bcc (a) MEA Ti-25Nb-25Zr-25Ta and HEA Ti-20Nb-20Zr-20Ta-20Mo equimassic alloys (b) materials coated with the MAO oxide, illustrating the thickness of the coatings.

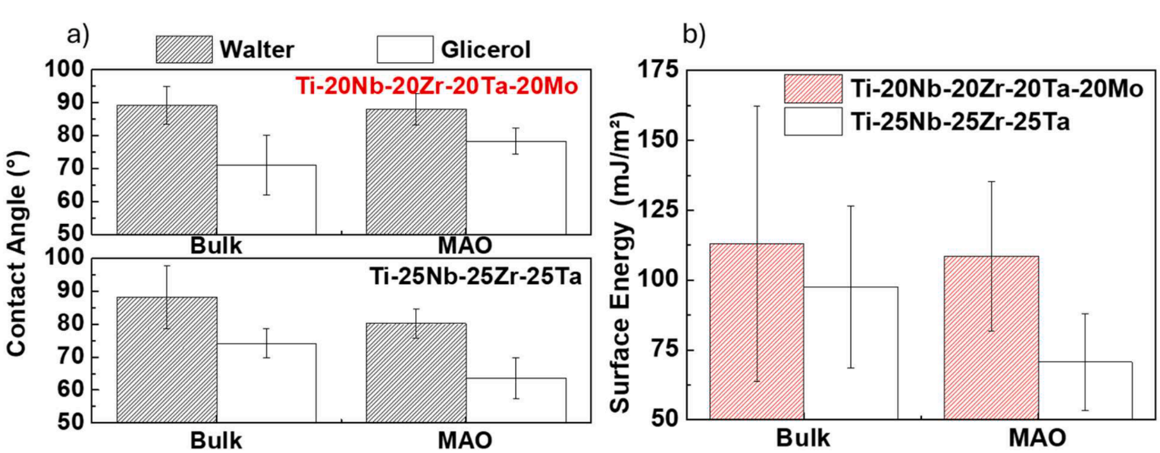

Fig. 5. Results of wettability (a) and surface energy (b) of the MEA Ti-25Nb-25Zr-25Ta and HEA Ti-20Nb-20Zr-20Ta-20Mo equimassic alloys produced in this study.

Fig. 5 presents the results of contact angle and surface energy. The metallic substrates of the alloys and the MAO coating are hydrophilic, with a contact angle (Θ) for both water and glycerol (as a polar liquid) being less than 90° The MAO surface exhibits a lower surface energy compared to that of the metallic substrate.

In all study conditions, the contact angle of the polar liquid (water) is greater than that of the nonpolar liquid (glycerol), indicating that the metallic surfaces of the Ti alloys and the MAO coating are nonpolar. There are no significant changes in the contact angle of the metallic bulk and the MAO coating; however, on the MAO surface of the quaternary alloy (Ti-25Nb-25Zr-25Ta), there is a slight decrease in wettability values compared to the MAO surface of the quinary alloy (Ti-20Nb-20Zr-20Ta-20Mo). This slight divergence is attributed to the shape of the anodic pores. The Ti-20Nb-20Zr-20Ta-20Mo alloy has smaller circular pores, while the Ti-25Nb-25Zr-25Ta alloy has larger lamellar pores (Fig. 5). When a droplet of liquid is placed on the MAO surface, atmospheric air may become trapped within the pores, resulting in an increased contact angle. The MAO surface of the Ti-20Nb-20Zr-20Ta-20Mo alloy features smaller pores, facilitating the entrapment of atmospheric air when the droplet is applied to its surface. In contrast, the MAO surface of the Ti-25Nb-25Zr-25Ta alloy contains lamellar structures that promote liquid penetration, resulting in a decreased contact angle.

The roughness of the MAO coatings was determined using confocal microscopy, revealing that the surface of the Ti-20Nb-20Zr-20Ta-20Mo alloy has a roughness (RMS) value of 1.6 ± 0.1 μm. In contrast, the MAO layer of the Ti-25Nb-25Zr-25Ta alloy exhibits a roughness (RMS) of 2.9 ± 0.4 μm. This study established that roughness is inversely proportional to the contact angle and surface energy, as the rougher surface displayed lower values of both contact angle and surface energy.

Fig. 6 presents a graphical representation of the Vickers microhardness variation for the alloys studied in this work. The observed increase in hardness, from (323 ± 7 HV) for Ti-25Nb-25Zr-25Ta alloy to (453 ± 10 HV) for Ti-20Nb-20Zr-20Ta-20Mo alloy, is closely associated with the integration of new elements, specifically the combination of Ta with Mo in the quaternary and quinary alloys. The addition of these elements affects not only bond strength but also the development and volume of phases present in the material. Moreover, solid solution hardening induces lattice distortions that impede dislocation movement and contribute to changes in microhardness [4–6]. Phase boundaries and these distortions act as obstacles to dislocations, further influencing hardness. These changes are characteristic of increased configurational entropy. Regarding the hardness of the MAO coating, a similar behavior is observed, with an increase in hardness attributed to the presence of Mo, which hardens the anodic film.

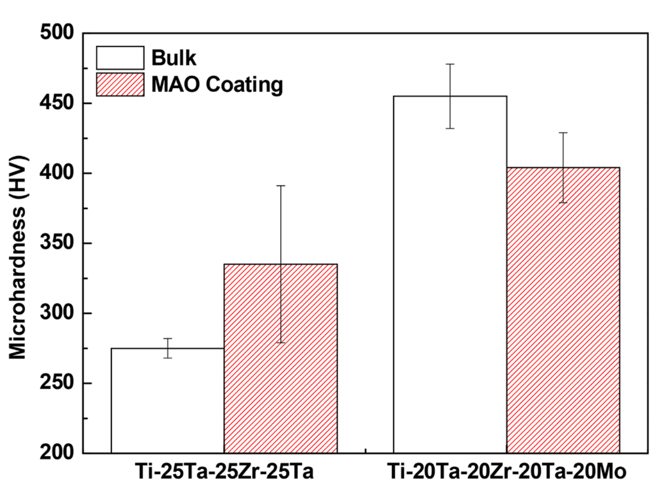

Fig. 6. Results of Vickers microhardness obtained on the metallic substrate and the MAO coating of the multiprincipal MEA Ti-25Nb-25Zr-25Ta and HEA Ti-20Nb-20Zr-20Ta-20Mo equimassic alloys.

Fig. 7 shows the results of cellular viability for the materials produced before and after the MAO process. All alloys in the studied systems, both with and without the MAO coating, exhibited absorbance values above the positive control, demonstrating that the cells remained viable after contact with the materials. Cellular viability refers to the ability of cells to maintain their vital functions; thus, the higher the absorbance value, the greater the percentage of live cells.

Fig. 8 shows the results of cellular adhesion of cells in contact with metallic alloys before and after the MAO process. In a manner analogous to the cellular viability results, the adhesion results show values greater than the control, indicating that the cells attached to and positively interacted with the surfaces of the materials.

It is noted that the quaternary alloy exhibits better biocompatibility results compared to the quinary alloy. Studies have shown a slight cytotoxic characteristic of the element Mo when in contact with the human body. The Ti-20Nb-20Zr-20Ta-20Mo alloy contains Mo in its chemical composition, and consequently, a small amount of Mo is also present in the MAO coating. As a result, the Ti-25Nb-25Zr-25Ta alloy, which does not contain Mo, shows improved viability and cellular adhesion results.

The scientific community continues to debate Mo's cytotoxicity. Some studies report a slight cytotoxic effect, which may reduce the biocompatibility of implants containing this element in their chemical composition. Other elements, such as Al, V, Ni, and Cr, also exhibit cytotoxicity.

Some studies in the literature report that metallic biomaterials should not have an absorbance value below 70% for both the adhesion and cellular viability assays, as low absorbance indicates cell death and poor adhesion of osteoblastic cells to the implants. The 70% threshold is established in the scientific community and standardized by ISO 10,993–5 [52]. Overall, it is observed that all alloys in the studied system, both with and without the MAO coating, exhibited cellular absorbance values above the positive control, indicating that they do not possess cytotoxic characteristics during the 24-hour period of contact with pre-osteoblastic cells.

4. Conclusions

Drawing from both the existing literature and the findings discussed in this study, the following key conclusions contribute to advancements in this field:

- Lattice parameters showed a smaller value for HEA Ti-20Nb-20Zr-20Ta-20Mo (a = 3.31 Å) against the value for MEA Ti-25Nb-25Zr-25Ta (a = 3.36 Å), attributed to Mo's smaller atomic radius and its influence on microstructural characteristics and hardness (β-Ti alloys);
- Micro-arc oxidation (MAO) yielded predominantly amorphous coatings, with the MEA multiprincipal Ti-25Ta-25Nb-25Zr alloy presenting a crystalline ZrO_2 phase, facilitated by the high voltage and current applied;
- The thickness of the MAO coating on the MEA quaternary alloy Ti-25Ta-25Nb-25Zr (10.4 μm) was greater than that on the HEA quinary alloy Ti-20Zr-20Ta-20Nb-20Mo (4.2 μm).
- Surface morphology analysis showed that multiprincipal HEA quinary Ti-20Nb-20Zr-20Ta-20Mo showed micropores, while MEA quaternary Ti-25Ta-25Nb-25Zr displayed lamellar porous structures advantageous for bone cell attachment, and contact angle tests confirmed hydrophilic surfaces with reduced surface energy on MAO coatings due to their structural characteristics
- The greater surface roughness on MEA quaternary Ti-25Ta-25Nb-25Zr contributes to lower contact angles and improved cell adhesion.
- Cell viability and adhesion tests partially infer their biocompatibility, with MEA multiprincipal Ti-25Ta-25Nb-25Zr exhibiting superior performance due to its Mo-free composition, and both alloys

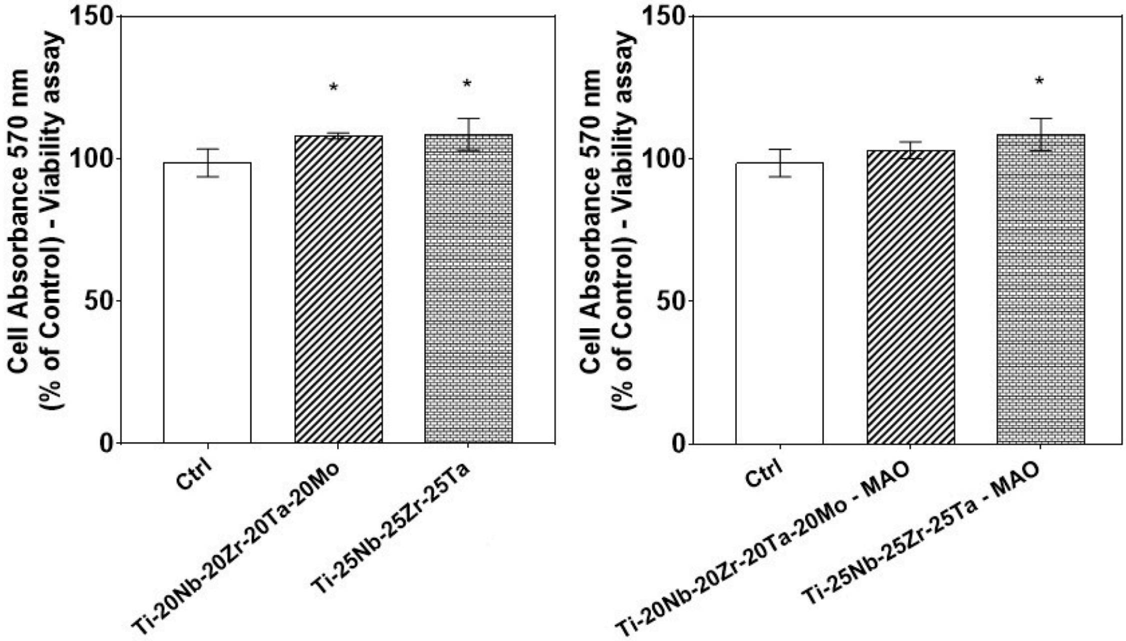

Fig. 7. Comparison of the cell viability assay considering the control group and the MEA Ti-25Nb-25Zr-25Ta and HEA Ti-20Nb-20Zr-20Ta-20Mo equimassic alloys.

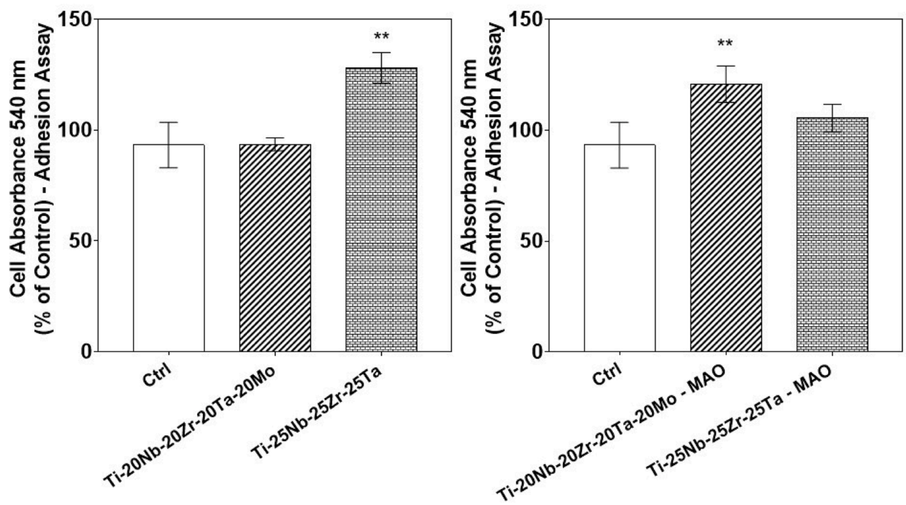

Fig. 8. Comparison of the cell adhesion assay considering the control group and the MEA Ti-25Nb-25Zr-25Ta and HEA Ti-20Nb-20Zr-20Ta-20Mo equimassic alloys.

surpassed ISO standards, underscoring their suitability for biomedical applications while highlighting Mo's mild cytotoxicity as a design consideration.

- Considering all the data, these findings suggest that the optimized MEA alloys have strong potential for use in biomedical applications mainly due to their favorable combination of mechanical properties, surface roughness, and biocompatibility, surpassing ISO standards for cellular viability and adhesion.

CRediT authorship contribution statement

Rafael F.M. dos Santos: Writing – original draft, Data curation. **Pedro A.B. Kuroda:** Writing – original draft, Formal analysis, Data curation. **Gerson S. de Almeida:** Writing – review & editing, Methodology, Investigation, Data curation. **Willian F. Zambuzzi:** Writing – review & editing, Methodology. **Carlos R. Grandini:** Writing – review & editing, Investigation. **Conrado R.M. Afonso:** Writing – review & editing, Supervision, Funding acquisition.

Declaration of competing interest

The authors declare that they have no known competing financial interests or personal relationships that could have appeared to influence the work reported in this paper.

Acknowledgement

The authors would like to thank Brazilian agencies CNPq PQ Grant # 310802/2023–7 (C.R.M.A.), CNPq Project Grant # 314.810/2021–8 (C.R.G.), CNPq Grant # 421.677/2023–6 (C.R.G.), CAPES Grant # 88881.310568/2018–01 (C.R.G.), CAPES financial code 001 and Grant # 88887.371759/2019–00 (R.F.M.S.), FAPESP "Projeto Temático" # 2018/18293–8, FAPESP-PAIP # 2023/16836–2, FAPESP-BPE Grant # 2024/05313–1 (C.R.M.A.), .FAPESP Grant # 2022/15157–1 (W.F.Z.), FAPESP Grant # 2024/203886–4 (G.S.A.), and FAPESP Post-Doctoral fellow Grant # 2019/26517–6 (P.A.B.K.) for their financial support.

Data availability

Data will be made available on request.

References

[1] B.D. Ratner, A.S. Hoffman, F.J. Schoen, J.E. Lemons, Biomaterials science: an Introduction to Materials in Medicine, Elsevier, 2004.
[2] J. Park, R.S. Lakes, Biomaterials an introduction - metallic implant materials. Biomaterials, Springer New York, New York, NY, 2007, pp. 99–137.
[3] L.-Y. Chen, Y.-W. Cui, L.-C. Zhang, Recent development in beta titanium alloys for biomedical applications, Metals. (Basel) 10 (2020) 1139.
[4] E. Alabort, Y.T. Tang, D. Barba, R.C. Reed, Alloys-by-design: a low-modulus titanium alloy for additively manufactured biomedical implants, Acta Mater. 229 (2022) 117749.
[5] N. Kumar, G.N. Arora, B. Datta, Bearing surfaces in hip replacement - Evolution and likely future, Med. J. Armed. Forces India 70 (2014) 371–376.
[6] M. Abdel-Hady Gepreel, M. Niinomi, Biocompatibility of Ti-alloys for long-term implantation, J. Mech. Behav. Biomed. Mater. 20 (2013) 407–415.
[7] S. Kurtz, K. Ong, E. Lau, F. Mowat, M. Halpern, Projections of primary and revision hip and knee arthroplasty in the United States from 2005 to 2030, J Bone Joint Surg. Am. 89 (2007) 780–785.
[8] E. Marin, A. Lanzutti, Biomedical applications of titanium alloys: a comprehensive review, Materials. (Basel) 17 (2024) 114.
[9] G. Li, F. Ma, P. Liu, S. Qi, W. Li, K. Zhang, X. Chen, Review of micro-arc oxidation of titanium alloys: mechanism, properties and applications, J. Alloys. Compd. 948 (2023) 169773.
[10] P. Pesode, S. Barve, A review—Metastable β titanium alloy for biomedical applications, J. Engineer. Appl. Sci. 70 (2023) 25.
[11] A.A. Elhadad, L. Romero-Resendiz, M.C. Rossi, L.M. Rodríguez-Albelo, S. Lascano, C.R.M. Afonso, A. Alcudia, V. Amigó, Y. Torres, Findings and perspectives of β-Ti alloys with biomedical applications: exploring beyond biomechanical and biofunctional behaviour, J. Mater. Res. Technol. 33 (2024) 3550–3618.
[12] S.-P. Wang, J. Xu, TiZrNbTaMo high-entropy alloy designed for orthopedic implants: as-cast microstructure and mechanical properties, Mater. Sci. Engineer. 73 (2017) 80–89.
[13] Y. Yuan, Y. Wu, Z. Yang, X. Liang, Z. Lei, H. Huang, H. Wang, X. Liu, K. An, W. Wu, Z. Lu, Formation, structure and properties of biocompatible TiZrHfNbTa high-entropy alloys, Mater. Res. Lett. 7 (2019) 225–231.
[14] M. Akmal, A. Hussain, M. Afzal, Y.I. Lee, H.J. Ryu, Systematic study of (MoTa) xNbTiZr medium- and high-entropy alloys for biomedical implants- In vivo biocompatibility examination, J. Mater. Sci. Technol. 78 (2021) 183–191.
[15] M. Niinomi, M. Nakai, Titanium-based biomaterials for preventing stress shielding between implant devices and bone, Int. J. Biomater. 2011 (2011) 836587.
[16] P.A.B. Kuroda, R.F.M. dos Santos, C.R. Grandini, C.R.M. Afonso, Unveiling the effect of Nb and Zr additions on microstructure and properties of β Ti-25Ta alloys for biomedical applications, Mater. Charact. 207 (2024) 113577.
[17] P.A.B. Kuroda, C.R. Grandini, C.R.M. Afonso, Structural characterization of the hot-rolled Ti-25Ta-xZr alloys by rietveld method, Mater. Res. 26 (2023).
[18] P.A.B. Kuroda, R.F.M. dos Santos, M.C. Rossi, D.R.N. Correa, C.R. Grandini, C.R. M. Afonso, Influence of Zr addition in β Ti-25Ta-xZr alloys on oxide formation by MAO-treatment, Vacuum. 217 (2023) 112541.
[19] R.F.M.d. Santos, P.A.B. Kuroda, C.N. Reis, C.R.M. Afonso, Influence of hot rolling on β Ti-Nb-Zr(-Ta) multiprincipal alloys for biomedical application, Mater. Res. 26 (2023).
[20] V.T. Nguyen, M. Qian, Z. Shi, T. Song, L. Huang, J. Zou, A novel quaternary equiatomic Ti-Zr-Nb-Ta medium entropy alloy (MEA), Intermetallics. 101 (2018) 39–43.
[21] M. Wong, J. Eulenberger, R. Schenk, E. Hunziker, Effect of surface topology on the osseointegration of implant materials in trabecular bone, J. Biomed. Mater. Res. 29 (1995) 1567–1575.
[22] M. Kobayashi, S. Nihonmatsu, T. Okawara, H. Onuki, H. Sakagami, H. Nakajima, H. Takeishi, J. Shimada, Adhesion and proliferation of osteoblastic cells on hydroxyapatite-dispersed Ti-based composite plate, In. Vivo (Brooklyn) 33 (2019) 1067–1079.
[23] M. Levin, R.C. Spiro, H. Jain, M.M. Falk, Effects of titanium implant surface topology on bone cell attachment and proliferation in vitro, Med. Devices (Auckl) 15 (2022) 103–119.
[24] S. Spriano, S. Yamaguchi, F. Baino, S. Ferraris, A critical review of multifunctional titanium surfaces: new frontiers for improving osseointegration and host response, avoiding bacteria contamination, Acta Biomater. 79 (2018) 1–22.
[25] P. Wan, W. Wang, L. Zheng, L. Qin, K. Yang, One-step electrodeposition synthesis of bisphosphonate loaded magnesium implant: a strategy to modulate drug release for osteoporotic fracture healing, J. Mater. Sci. Technol. 78 (2021) 92–99.
[26] G.C. Cardoso, C.R. Grandini, J.V. Rau, Comprehensive review of PEO coatings on titanium alloys for biomedical implants, J. Mater. Res. Technol. 31 (2024) 311–328.
[27] P.A.B. Kuroda, G.C. Cardoso, M.C. Rossi, C.R.M. Afonso, C.R. Grandini, Structural and morphological modification of the PEO coating on the Ti-25Ta-10Zr-15Nb alloy through heat treatment, Mater. Lett. 373 (2024) 137155.
[28] V.P. Ricci, R.F.M. dos Santos, G.H. Asato, V. Roche, A.M. Jorge, C.R.M. Afonso, Assessment of anodization conditions and annealing temperature on the microstructure, elastic modulus, and wettability of β-Ti40Nb alloy, Thin. Solid. Films. 737 (2021) 138949.
[29] M. Aliofkhazraei, D.D. Macdonald, E. Matykina, E.V. Parfenov, V.S. Egorkin, J. A. Curran, S.C. Troughton, S.L. Sinebryukhov, S.V. Gnedenkov, T. Lampke, F. Simchen, H.F. Nabavi, Review of plasma electrolytic oxidation of titanium substrates: mechanism, properties, applications and limitations, Appl. Surface Sci. Adv. 5 (2021) 100121.
[30] J. Zhang, W. Dai, X. Wang, Y. Wang, H. Yue, Q. Li, X. Yang, C. Guo, C. Li, Micro-arc oxidation of Al alloys: mechanism, microstructure, surface properties, and fatigue damage behavior, J. Mater. Res. Technol. 23 (2023) 4307–4333.
[31] S. Sikdar, P.V. Menezes, R. Maccione, T. Jacob, P.L. Menezes, Plasma electrolytic oxidation (PEO) process-processing, Properties, and Applications, Nanomaterials (Basel, Switzerland) 11 (2021).
[32] B. Makurat-Kasprolewicz, A. Ossowska, Recent advances in electrochemically surface treated titanium and its alloys for biomedical applications: a review of anodic and plasma electrolytic oxidation methods, Mater. Today Commun. 34 (2023) 105425.
[33] P.A.B. Kuroda, F.N. de Mattos, C.R. Grandini, C.R.M. Afonso, Micro-abrasive wear behavior by ball cratering on MAO coating of Ti-25Ta alloy, J. Mater. Res. Technol. (2023).
[34] P.A.B. Kuroda, M.C. Rossi, C.R. Grandini, C.R.M. Afonso, Assessment of applied voltage on the structure, pore size, hardness, elastic modulus, and adhesion of anodic coatings in Ca-, P-, and Mg-rich produced by MAO in Ti–25Ta–Zr alloys, J. Mater. Res. Technol. 26 (2023) 4656–4669.
[35] P.A.B. Kuroda, G.C. Cardoso, M.C. Rossi, C.R. Grandini, C.R.M. Afonso, Effect of the incorporation of bactericidal agents Ag, Cu, and Zn through micro-arc oxidation on the properties of the Ti-25Ta alloy surface, Mater. Res. 27 (2024).
[36] G.C. Cardoso, K. Barbaro, P.A. Kuroda, A. De Bonis, R. Teghil, V. Monteleone, L. Imperatori, M. Ortenzi, I. Antoniac, C.R. Grandini, J.V. Rau, Silver Containing Antimicrobial Coatings on Innovative Ti-30Nb-5Mo β-Alloy Prepared By Micro-Arc Oxidation For Biomedical Implant Applications, Coatings, 2024.
[37] G.C. Cardoso, K. Barbaro, P.A.B. Kuroda, A. De Bonis, R. Teghil, I.I. Krasnyuk, L. Imperatori, C.R. Grandini, J.V. Rau, Antimicrobial Cu-Doped TiO2 Coatings on the β Ti-30Nb-5Mo Alloy by Micro-Arc Oxidation, Materials. (Basel) 17 (2024) 156.
[38] G.C. Cardoso, K. Barbaro, P.A.B. Kuroda, L. Imperatori, A. De Bonis, R. Teghil, M. Curcio, E. Innocenzi, V.Y. Grigorieva, G. Vadalà, C.R. Grandini, J.V. Rau, Incorporation of Ca, P, Mg, and Zn elements in Ti-30Nb-5Mo alloy by micro-arc oxidation for biomedical implant applications: surface characterization, cellular growth, and microorganisms' activity, Coatings 13 (2023) 1577.
[39] R.F.M.d. Santos, P.A.B. Kuroda, C.R.M. Afonso, New low elastic modulus equimassic βeta Ti-Nb-Zr-(Ta-Mo) multiprincipal alloys, J. Alloys Compounds Commun. 4 (2024) 100040.
[40] P.A.B. Kuroda, C.R. Grandini, C.R.M. Afonso, Surface characterization of new β Ti-25Ta-Zr-Nb alloys modified by micro-arc oxidation, Materials. (Basel) 16 (2023) 2352.
[41] G. Zhang, Y. Chen, Y. Cao, B. Liu, Q. Huang, Y. Liu, Superior self-lubricating coatings with heterogeneous nanocomposite structures on Ti–Nb–Zr–Ta–Hf refractory multi-principal element alloy, Adv. Funct. Mater. 34 (2024) 2405657.
[42] G. Zhang, S. Huang, X. Li, D. Zhao, Y. Cao, B. Liu, Q. Huang, Oxide ceramic coatings with amorphous/nano-crystalline dual-structures prepared by micro-arc oxidation on Ti–Nb–Zr medium entropy alloy surfaces for biomedical applications, Ceram. Int. 49 (2023) 18114–18124.
[43] M. Fellah, N. Hezil, D. Bouras, M.A. Habeeb, F. Hamadi, N. Bouchareb, S. E. Laouini, A. Perez Larios, O. Aleksei, G.A. El-Hiti, Microstructural and photocatalytic properties of nanostructured near-β Ti-Nb-Zr alloy for total hip prosthesis use, Kuwait J. Sci. 51 (2024) 100276.
[44] P.A.B. Kuroda, F.d.F. Quadros, M.V. Nascimento, C.R. Grandini, Development and characterization of new Ti-25Ta-Zr alloys for biomedical applications, Mater. Sci. Forum 1016 (2021) 137–144.
[45] P.A.B. Kuroda, B.L.T. Pedroso, F.M.L. Pontes, C.R. Grandini, Effect of titanium addition on the structure, microstructure, and selected mechanical properties of As-Cast Zr-25Ta-xTi Alloys, Metals. (Basel) 11 (2021) 1507.
[46] P.A.B. Kuroda, T.H. Montes, M.C. Rossi, C.R. Grandini, C.R.M. Afonso, Unraveling crystalline phases, morphology, hardness, and adhesion of PEO anodic coatings on Ti-15Nb alloy surface, Mater. Lett. 356 (2024) 135607.
[47] E. ASTM, 92–82. Standard test method for vickers hardness of metallic materials, annual book of ASTM standards (reapproved 2003), 3 (2003) 1–9.
[48] M.C. Rossi, R.F. dos Santos, P.A.B. Kuroda, C.R.M. Afonso, Characteristics of Ceramic-Like Coatings Obtained By Plasma Electrolyte Oxidation On Different Ti alloys, Boletín de la Sociedad Española de Cerámica y Vidrio, 2023.
[49] N. Attarzadeh, C.V. Ramana, Plasma electrolytic oxidation ceramic coatings on Zirconium (Zr) and ZrAlloys: part i—growth mechanisms, microstructure, and chemical composition, Coatings 11 (2021) 634.
[50] I.D. Muhammad, M. Awang, Modelling the interatomic potential of cubic zirconia, Appl. Mech. Mater. 446-447 (2014) 151–157.
[51] R.A. Ploc, The lattice parameter of cubic ZrO2 formed on zirconium, J. Nuclear Mater. 99 (1981) 124–128.
[52] I. 10993, Biological evaluation of medical devices. Part 5: Test for cytotoxicity: in Vitro Methods, International Organization for Standardization, Genebra (Sweden), 2005.